QUANTITATIVE DESCRIPTION OF THE SODIUM CONDUCTANCE OF THE GIANT AXON OF *MYXICOLA* IN TERMS OF A GENERALIZED SECOND-ORDER VARIABLE

L. GOLDMAN

From the Department of Physiology, School of Medicine, University of Maryland, Baltimore, Maryland 21201

ABSTRACT A variety of experimental observations in *Myxicola* and other preparations indicate that the sodium conductance, g_{Na}, has properties quite different from those described by the m and h variables of Hodgkin and Huxley. A new quantitative description of the g_{Na} is presented in which the g_{Na} is assumed to be proportional to the fifth power of a generalized second-order variable, i.e., $g_{Na} = \bar{g}'_{Na} \nu^5$, $\dot{\nu} = -K_1 \nu + K_2 U + K_3$, $\dot{U} = -K_4 U + K_5 \nu + K_6$. This model is shown to be able to quantitatively simulate all of the experimentally observed behavior of the g_{Na}. A view of the sodium gate consistent with these kinetics is to imagine it to be composed of five independent subunits, each of the type

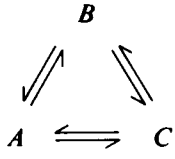

where A represents the resting state, B the conducting state, and C the inactivated state. A model in which the subunit is of the type $A \rightleftharpoons B \rightleftharpoons C$ could not simulate the experimental observations. It was concluded that two processes are sufficient to account for all of the behavior of the g_{Na}.

INTRODUCTION

If one does, in *Myxicola*, the same sorts of experiments on the sodium conductance (g_{Na}) that Hodgkin and Huxley did on the squid (Hodgkin and Huxley, 1952 *a*, *b*), one obtains similar results (Binstock and Goldman, 1969; Goldman and Binstock, 1969; Goldman and Schauf, 1972). However, there are a number of additional observations on *Myxicola*, and other preparations, which cannot be reconciled with the kinetics of the g_{Na} as proposed by Hodgkin and Huxley (1952 *c*), and which indicate that the g_{Na} is a different kind of system than that described by them.

In *Myxicola*, the h_∞ curve (the normalized peak value of the sodium current, I_{Na}, during a test pulse vs. the potential of a long lasting conditioning voltage clamp pulse) is a function of the g_{Na} during the test pulse, translating to the right along the voltage axis as the g_{Na} is increased (Goldman and Schauf, 1972). This effect, which was also reported in squid by Hoyt and Adelman (1970) and which may account for some of the variability in h_∞ curves seen in the node by Frankenhaeuser (1959), was qualitatively predicted by Hoyt (1968) based on an earlier (1963) analysis of squid voltage-clamp data in terms of a coupled activation-inactivation process. In Hodgkin-Huxley kinetics the h_∞ curve is a parameter and ought not to show this effect.

In *Myxicola* (Goldman and Schauf, 1972) there is an initial delay in the development of the inactivation of the g_{Na}, and also in the recovery from inactivation (Schauf, 1974). Such delays in the development of inactivation were first reported by Armstrong (1970) in *Dosidicus* axons, and have also been seen in the node (Peganov, 1973). In *Myxicola*, the delay is reduced if a larger conditioning pulse, with a more rapidly rising g_{Na}, is used (Goldman and Schauf, 1972), and this result has also been confirmed in the node (Peganov, 1973). Chandler et al. (1965) first suggested that delays in the development of inactivation might be expected if activation and inactivation are coupled, owing to the time taken for the development of the g_{Na} during the conditioning pulse. For Hodgkin-Huxley kinetics inactivation ought to be strictly exponential at all times.

In *Myxicola*, there is a range of nearly 50 mV over which the values for the time constant of inactivation, τ_h, fitted to the decay of the g_{Na} during test pulses, may be compared to values for the time constant of inactivation, τ_c, determined from the effects of conditioning pulses of different durations on the peak I_{Na} during a test pulse. When Goldman and Schauf (1973) compared their τ_h values to the τ_c data of Goldman and Schauf (1972), τ_c values were found to be considerably larger at every potential. It seems likely that a similar effect can be seen in frog atria (Haas et al., 1971). These results indicate that the process governing the shut off of the g_{Na} during a test pulse is not identical to that observed from the effects of depolarizing conditioning pulses. For Hodgkin-Huxley kinetics the two time constants ought to be the same. For conditioning pulse durations long relative to the time constant of activation, the effects of further increases of conditioning pulse duration should have been expressed only as changes of the initial value of the inactivation variable, h_0, at the start of the test pulse. For coupled activation-inactivation kinetics, the two time constants are not required to be the same as they do not represent the same process, i.e. τ_h would reflect the net draining of the conducting state and τ_c the changes in time of the extent to which the conducting state can be filled from a resting state.

Goldman and Schauf (1973) also compared steady-state values of the Hodgkin-Huxley inactivation variable, h_∞, fitted to the g_{Na} during test pulses, to those determined with long-lasting conditioning pulses. h_∞ values fitted to the time course of the g_{Na} were never reliably different from zero even at potentials where the h_∞ curve had a value of 0.5. These results indicate that there is a range of conditioning pulses for

which, for at least some test pulses, the following sequence can be observed: the g_{Na} during the conditioning pulse rises up and then declines to nearly zero, while during the immediately subsequent test pulse, the g_{Na} again rises up and again declines to near zero. In Hodgkin-Huxley kinetics, the inactivation variable is a monotonic function of potential, and of time at any fixed potential. These results rule out any model in which the g_{Na} is governed by the product of two independent first-order variables.

There are other observations available which bear on models for the g_{Na}. In the node, Frankenhaeuser (1963) found that the τ_h during a fixed test pulse could be affected by conditioning polarization. This dependency of τ_h on initial conditions seems to be the first observation of a serious discrepancy with Hodgkin-Huxley kinetics, and is of itself inconsistent with the Hodgkin-Huxley first order inactivation variable. More recently, Chandler and Meves (1970) working on squid axons internally perfused with NaF solutions have reported several inactivation phenomena which are also not reconcilable with Hodgkin-Huxley kinetics.

These results all indicate that the physical processes underlying the g_{Na} are not adequately described by the m and h variables of Hodgkin and Huxley (1952 *c*), and that a new quantitative approach will be needed. The first question that one might ask in such an analysis is whether this complex array of behavior exhibited by the g_{Na} can be reproduced by any model consisting of only two variables (either coupled or independent), i.e. whether only two processes are sufficient. In this paper a quantitative description of the g_{Na} in *Myxicola* in terms of a generalized second order variable is presented. It will be shown that this model can quantitatively simulate all of the experimentally observed behavior, and that two processes are indeed sufficient.

DESCRIPTION OF THE MODEL AND RESULTS

No new data are presented in this paper, rather the data of Goldman and Schauf (1972, 1973), which have previously been analyzed in terms of Hodgkin-Huxley kinetics, are here reanalyzed in terms of a new kinetic model.

The open circles in Fig. 1 indicate experimental values of the g_{Na} as a function of time, under voltage clamp, for each of the clamped potentials indicated. These data are from the same axon illustrated in Fig. 9 of Goldman and Schauf (1973). The solid lines have been computed from

$$g_{Na} = \bar{g}'_{Na} \nu^5, \tag{1}$$

where ν is defined by the general second-order differential equation,

$$\ddot{\nu} + (a + b)\dot{\nu} + ab(\nu - \nu_\infty) = 0, \tag{2}$$

and a, b, and ν_∞ are functions of membrane potential only. $\bar{g}'_{Na}$ is a constant with the units of conductance, and may be interpreted as the product of the conductance of a channel when maximally conducting, the channel density and an unknown scaling factor on ν. Table I gives the $\bar{g}'_{Na}$ values for each of the five axons analyzed.

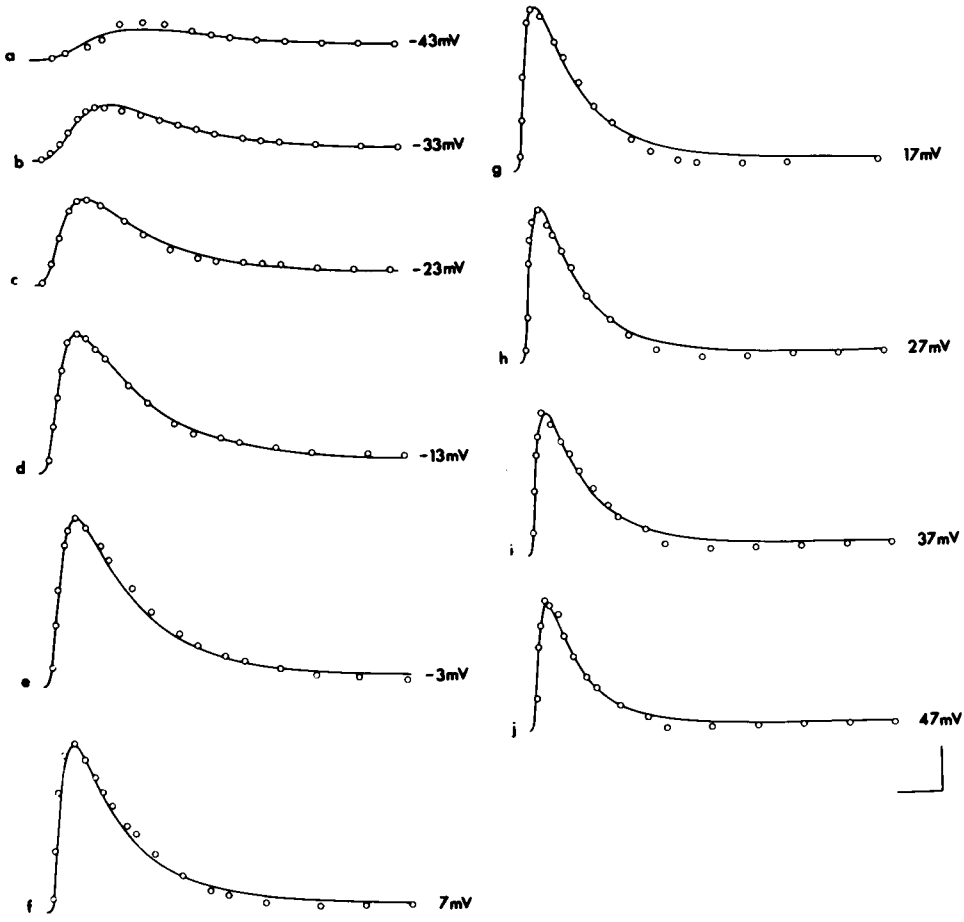

FIGURE 1 Experimental values of the sodium conductance (open circles) as a function of time, recorded under voltage clamp, for each of the clamp potentials indicated. The solid lines have been computed from Eqs. 1 and 3 in the text. Scale: *a*, *b*, 3 mmho/cm^2, *c–j*, 5 mmho/cm^2, 1 ms.

TABLE I
COLLECTED $\bar{g}'_{Na}$ VALUES

Axon	$\bar{g}'_{Na}$
	mmho/cm^2
71M29	38.5
71M31	37.2
71M32	46.2
71M33	43.6
71M34	33.4
Mean	39.8

TABLE II

CONSTANTS USED TO COMPUTE THE g_{Na} CURVES OF FIG. 1

V	a	b	ν_∞	$\dot{\nu}^*(0)$
mV	ms^{-1}	ms^{-1}		ms^{-1}
−43	1.249	0.1227	0.20	0.8020
−33	1.686	0.1943	0.25	1.2569
−23	2.813	0.2372	0.35	2.4016
−13	3.807	0.2188	0.35	3.4852
− 3	4.406	0.2526	0.35	4.2001
7	5.130	0.3003	0.35	4.8863
17	5.971	0.3560	0.35	5.6838
27	6.182	0.4094	0.35	5.8582
37	7.121	0.3993	0.35	6.5256
47	7.682	0.5081	0.35	6.9929

$\bar{g}'_{Na}$ is 43.62 mmho/cm^2. $\nu(0)$ is 0.

For a step in potential rising instantaneously at time zero, a solution to Eq. 2 is readily obtained:

$$\nu = \nu_\infty - \left[\frac{\dot{\nu}(0) + b(\nu(0) - \nu_\infty)}{a - b}\right] e^{-at} + \left[\frac{\dot{\nu}(0) + a(\nu(0) - \nu_\infty)}{a - b}\right] e^{-bt}, \tag{3}$$

where t is time, $\nu(0)$ is the initial value of ν at $t = 0$, and $\dot{\nu}(0)$ is the initial velocity. Eq. 3 is the expression actually fitted to the data of Fig. 1, and Table II shows the individual values used to compute each of the curves of Fig. 1. Models of the sort indicated by Eq. 2 were first proposed by Hodgkin and Huxley (1952 *c*) and further considered by Hoyt (1963, 1968).

Eq. 1 was not obtained by assuming a power function. Rather, it was assumed only that g_{Na} is some function of ν, and the experimental data were allowed to define this function, using the procedure described by Hoyt (1963). As a first approximation, it was assumed that g_{Na} was an exponential function of ν. This first approximation gave an adequate fit to the time course of the g_{Na} for a small depolarizing step (−33 mV), i.e. both $(\nu - \nu_\infty)$ vs. t, for long times, and $(-\nu + \nu_\infty + [(\dot{\nu}(0) - a\nu_\infty)/(a - b)] \cdot e^{-bt})$ vs. t were found to be reasonably linear on a semi-log plot.

When this analysis was applied to a wider range of ν values by examining a larger depolarizing step (−3 mV), linear plots were not obtained, indicating that an exponential relation is inadequate. However both for very small and very large values of t, where ν is small, linear plots are obtained, values for the parameters a, b, ν_∞, and $\dot{\nu}(0)$ can be determined, and a predicted $\nu(t)$ is obtained from the extrapolated straight line. By making a point by point in time comparison of the predicted $\nu(t)$ to the experimental $g_{Na}(t)$, a relationship between g_{Na} and ν is constructed, which both fits the experimental observations and is self consistent (i.e. the appropriate linear semi-log

plots are obtained). The resultant curve was found to be well described by a power function of order five, neither four nor six being adequate. The discovery of Eq. 1, itself constitutes one of the new results of this paper.

Describing the g_{Na} during a test pulse is a necessary criterion that any model must satisfy, but is not of itself a critical test of the model. A model for the g_{Na} must be able to provide a single set of parameters which account quantitatively for both the time course of the g_{Na} during any test pulse, and simultaneously for the effects of conditioning pulses of various potentials and durations on the g_{Na} during a test pulse.

Eq. 3 is written in terms of the four parameters a, b, ν_∞, and $\dot{\nu}(0)$ (or $\dot{\nu}^*(0)$, see below). The pooled values for these parameters for each of the five axons analysed are shown by the open circles in Fig. 2. a, b, and ν_∞ depend only on the test pulse potential. However, $\dot{\nu}(0)$ depends both on the test pulse potential and on the initial conditions, i.e. on what the potential was before the test step and on how long it was at that potential. To calculate the effects of conditioning pulses, therefore, it is convenient to replace the second-order differential equation (Eq. 2) with the following pair of coupled first-order differential equations:

$$\dot{\nu} = -K_1 \nu + K_2 U + K_3 \tag{4}$$

$$\dot{U} = -K_4 U + K_5 \nu + K_6, \tag{5}$$

where K_1 to K_6 are functions of membrane potential only. Any number of pairs of coupled equations could have been selected, Eqs. 4 and 5 being completely generalized.

The form of Eqs. 4 and 5 is consistent with the view that the conductance variable represents a process of the type in Scheme I:

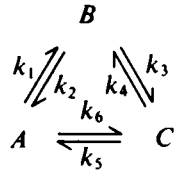

where A represents the resting state, B represents the conducting state, and C represents the inactivated state. Defining

$$\nu = [B]/([A] + [B] + [C]),$$

and

$$U = [C]/([A] + [B] + [C]),$$

the following relations obtain between the K's of Eqs. 4 and 5 and the molecular rate constants:

$$K_1 = k_1 + k_2 + k_3,$$
$$K_2 = k_4 - k_1,$$

$$K_3 = k_1,$$
$$K_4 = k_4 + k_5 + k_6,$$
$$K_5 = k_3 - k_6,$$
$$K_6 = k_6.$$

To implement the model, one needs, for each potential, the four terms which describe the time course of the g_{Na} (a, b, ν_∞, $\dot{\nu}(0)$) plus two values of $\dot{\nu}(0)$ for some other test pulse, used as a probe, at two different times, i.e. following two different durations at the original potential. The pooled conditioning pulse data of Goldman and Schauf (1972) were used to determine the two $\dot{\nu}(0)$ values for the probing pulse. Computations of the effects of conditioning pulses can then be made if the constants K_1 to K_6 can be defined in terms of these experimentally known terms.

It may be readily shown that it is not possible to uniquely define the six constants in Eqs. 4 and 5 this way. However, it is possible to uniquely define them if the additional assumption is made that the steady state is a true equilibrium state, i.e. that scheme I is not coupled to an energy source. In this case the condition that the net steady state flux between any two states in scheme I is zero, yields the following relation between the molecular rate constants:

$$k_2 k_4 k_6 = k_1 k_3 k_5, \tag{6}$$

and the number of unknown terms is reduced by one. However, the labor in extracting these constants is considerable. What is presented here is an interim computation in which the values of the molecular rate constants have not been determined and for which it is not necessary to know, e.g., the value of the scaling factor on ν. The purpose of this interim computation is to establish that the model can indeed quantitatively account for all of the experimentally observed behavior, both for test pulses and for the effects of conditioning pulses, before undertaking the labor of a more complete analysis.

To apply Eqs. 4 and 5 to a conditioning pulse experiment, consider any test (probing) pulse evaluated at $t = 0$, and any conditioning pulse. For any two durations of the conditioning pulse, t_{c1} and t_{c2},

$$\dot{\nu}(0)_1 = -K_1 \nu_{c1} + K_2 U_{c1} + K_3, \tag{7A}$$
$$\nu_{c1} = -K_{1c} \nu_{c1} + K_{2c} U_{c1} + K_{3c}, \tag{7B}$$
$$\dot{\nu}(0)_2 = -K_1 \nu_{c2} + K_2 U_{c2} + K_3, \tag{7C}$$
$$\dot{\nu}_{c2} = -K_{1c} \nu_{c2} + K_{2c} U_{c2} + K_{3c}. \tag{7D}$$

where the terms subscripted c refer to the conditioning pulse. Evaluating Eq. 4 at $t = 0$, and setting $U(0) = \nu(0) = 0$ we have

$$K_3 = \dot{\nu}^*(0), \tag{8A}$$

and similarly

$$K_{3c} = \dot{v}_c^*(0), \tag{8B}$$

where the starred values indicate the contribution to the initial velocity from the test step only.

U and v are probably never strictly zero, i.e., the A, B, and C states of scheme I are expected to have some non-zero occupancy at every potential. However, there is probably little error in assigning $[A]$ a value of unity when the g_{Na} has been fully primed, i.e. in the presence of long-lasting strong hyperpolarization, to a potential of −110 mV or less (Goldman and Schauf, 1972). The open circles of Fig. 2 D are

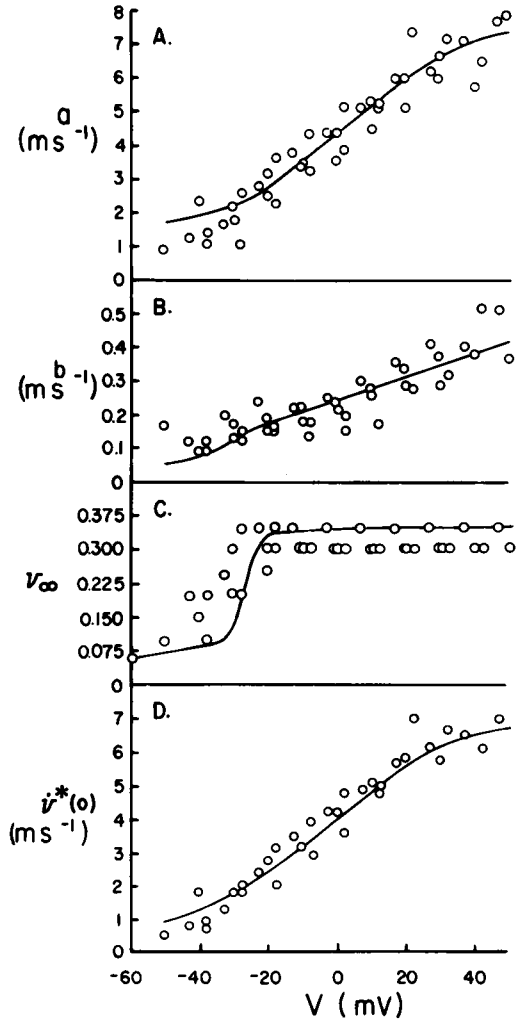

FIGURE 2 Values of the parameters used to fit a second order variable to the time course of the sodium conductance. Data pooled from five axons. The open circles indicate the values fitted to experimental records, and the solid lines indicate the smoothed values used for computations.

actually $\dot{\nu}^*(0)$ values obtained from the four axons in which each test step was preceded by a −50 mV conditioning step for 80 ms (Goldman and Schauf, 1973). The fifth axon (71M31) had a holding potential of −60 mV, without conditioning hyperpolarization, and its $\dot{\nu}(0)$ values are not included.

Eliminating U_{c1} between Eqs. 7 *A* and 7 *B*, and U_{c2} between Eqs. 7 *C* and 7 *D*, we have, after substituting from Eqs. 8 *A* and 8 *B* and rearranging, the following expressions:

$$\dot{\nu}(0)_1 = \alpha \nu_{c1} + \beta(\dot{\nu}_{c1} - \dot{\nu}_c^*(0)) + \dot{\nu}^*(0), \tag{9A}$$

$$\dot{\nu}(0)_2 = \alpha \nu_{c2} + \beta(\dot{\nu}_{c2} - \dot{\nu}_c^*(0)) + \dot{\nu}^*(0), \tag{9B}$$

where

$$\alpha = (K_2/K_{2c})K_{1c} - K_1,$$

and

$$\beta = K_2/K_{2c}.$$

Solving for α and β we obtain

$$\alpha = -\frac{\dot{\nu}(0)_1(\dot{\nu}_{c2} - \dot{\nu}_c^*(0)) + \dot{\nu}(0)_2(\dot{\nu}_c^*(0) - \dot{\nu}_{c1}) + \dot{\nu}^*(0)(\dot{\nu}_{c1} - \dot{\nu}_{c2})}{\nu_{c1}(\dot{\nu}_c^*(0) - \dot{\nu}_{c2}) + \nu_{c2}(\dot{\nu}_{c1} - \dot{\nu}_c^*(0))}, \tag{10}$$

$$\beta = \frac{\alpha \nu_{c2} + \dot{\nu}^*(0) - \dot{\nu}(0)_2}{\dot{\nu}_c^*(0) - \dot{\nu}_{c2}}, \tag{11}$$

where all the terms on the right hand side of Eqs. 10 and 11 are experimentally determined.

The effects of changes in initial conditions, then, may be computed using the following expressions: first for the conditioning pulse,

$$\nu_c = \nu_{c\infty} - \left[\frac{\dot{\nu}_c(0) + b_c(\nu_c(0) - \nu_{c\infty})}{a_c - b_c}\right] e^{-a_c t_c} + \left[\frac{\dot{\nu}_c(0) + a_c(\nu_c(0) - \nu_{c\infty})}{a_c - b_c}\right] e^{-b_c t_c}, \tag{12}$$

then to compute the $\dot{\nu}(0)$ of the test pulse,

$$\dot{\nu}(0) = \alpha \nu_c + \beta(\dot{\nu}_c - \dot{\nu}_c^*(0)) + \dot{\nu}^*(0), \tag{13}$$

and for the test pulse

$$\nu = \nu_\infty - \left[\frac{\dot{\nu}(0) + b(\nu_c - \nu_\infty)}{a - b}\right] e^{-at} + \left[\frac{\dot{\nu}(0) + a(\nu_c - \nu_\infty)}{a - b}\right] e^{-bt}. \tag{3}$$

TABLE III

INITIAL VELOCITIES FOR A 17 mV PROBING PULSE FOR EACH OF THE CONDITIONING PULSE POTENTIALS AND DURATIONS INDICATED

V	t_1	$\dot{\nu}(0)_1$	t_2	$\dot{\nu}(0)_2$
mV	ms	ms^{-1}	ms	ms^{-1}
− 5	3.0	0.175	80.0	0.0
−10	3.5	0.275	80.0	0.0
−15	4.0	0.415	80.0	0.0
−20	4.5	0.630	80.0	0.220
−25	5.5	1.080	80.0	0.920
−30	7.0	1.905	80.0	2.115
−35	10.0	2.410	80.0	2.783
−40	10.0	2.744	80.0	3.236
−45	15.0	3.220	80.0	3.661
−50	20.0	3.386	80.0	4.009

$\nu_c(0)$ is taken from the mean of the $\nu(0)$ values for each test pulse of axon 71M31. This method may be expanded to include computations of action potentials. For a test pulse j, a conditioning pulse i, and a reference test k, we have:

$$\alpha_{ij} = (\alpha_{ik} - \alpha_{jk})/\beta_{jk}$$

and

$$\beta_{ij} = \beta_{ik}/\beta_{jk}.$$

The solid lines in Fig. 2 indicate the smoothed values for the parameters selected for the computations presented in Figs. 3–9, and are not specifically fitted to the open circles. $\dot{\nu}(0)_1$, and $\dot{\nu}(0)_2$ values are shown in Tables III and IV.

The open circles in Fig. 3 indicate the experimental values of the normalized peak g_{Na} as a function of the test pulse potential. The solid line, which well describes the data, indicates the values computed using the smoothed values of Fig. 2. This is one of three criteria which indicate that the smoothed parameters of Fig. 2 satisfactorily

TABLE IV

INITIAL VELOCITIES OF THE INDICATED PROBING PULSES FOLLOWING A −10 mV, 3.5 ms CONDITIONING PULSE

V	$\dot{\nu}(0)_1$
mV	ms^{-1}
50	0.359
45	0.348
40	0.338
35	0.328
30	0.317
10	0.250
0	0.210

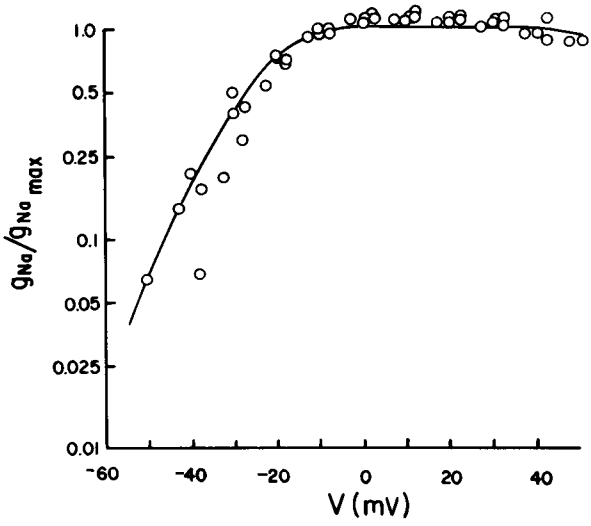

FIGURE 3 Peak value of the sodium conductance relative to the maximum value attained with any test pulse ($g_{Na}/g_{Na_{max}}$) as a function of test pulse potential (V). The open circles indicate the experimental values, and the solid line has been computed from Eqs. 1 and 3 using the smoothed parameters of Fig. 2.

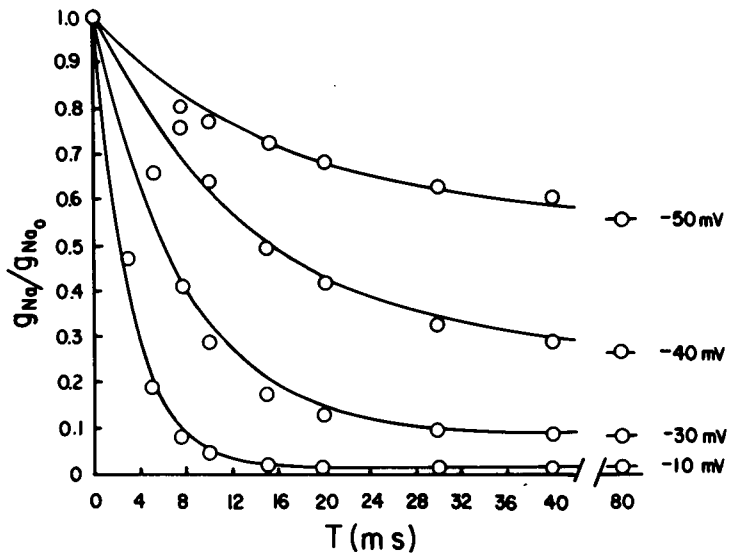

FIGURE 4 A simulated conditioning pulse experiment. The open circles are the computed peak values of the g_{Na} during a 17 mV test pulse, relative to the value with no conditioning pulse, as a function of conditioning pulse duration, for each of the conditioning pulse potentials indicated at the right. The solid lines have been computed from $g_{Na}/g_{Na_0} = (g_{Na}/g_{Na_0})_\infty - [(g_{Na}/g_{Na_0})_\infty - 1]e^{-t/\tau_c}$.

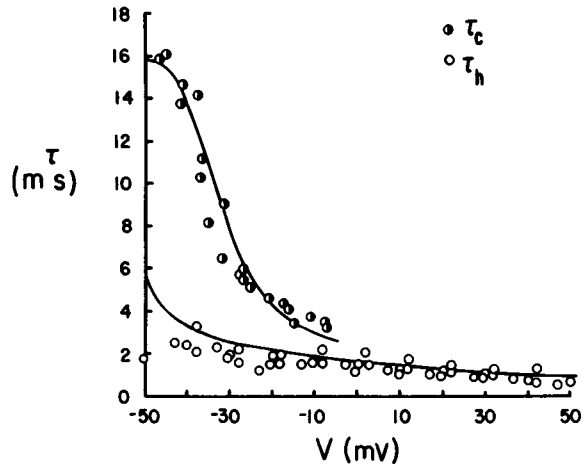

FIGURE 5 The open circles indicate the experimental values of the time constant of inactivation, τ_h, fitted to the decay of the g_{Na} during a test pulse, as a function of test pulse potential. The half-filled circles indicate the experimental values of the time constant of inactivation, τ_c, determined from the effects of conditioning pulses on the peak g_{Na} during a 17 mV test pulse, as a function of conditioning pulse potential. The solid lines have been computed as described in the text.

simulate the experimental test pulse data. A second criterion is the τ_h vs. test pulse data (Fig. 5, open circles and lower solid line), and the third is the fit of the solid lines to the open circles in Fig. 2 itself.

The open circles in Fig. 4 indicate the computed values of the peak g_{Na} during a 17 mV test pulse following conditioning pulses of the potentials and durations indicated. Peak g_{Na} values were computed for only a few representative durations of the conditioning pulse, and no attempt was made to interpolate between them. The behavior of the model is much like that of real axons, the decay of the peak g_{Na} being generally, but not strictly, exponential (see Goldman and Schauf, 1972, Fig. 1). The solid lines have been computed, in the manner of Hodgkin and Huxley, from the exponential

$$g_{Na}/g_{Na_0} = (g_{Na}/g_{Na_0})_\infty - [(g_{Na}/g_{Na_0})_\infty - 1]e^{-t/\tau_c}.$$

The τ_c values determined in this way are plotted as the upper solid line in Fig. 5 and the half-filled circles indicate the experimental values of Goldman and Schauf (1972). Both the τ_h and τ_c values are well predicted by the model.

The solid line in Fig. 6 is computed from the expression (Hodgkin and Huxley, 1952 *b*)

$$h_\infty = [1 + \exp([V_h - V]/k_h)]^{-1},$$

with a V_h of -51.5 mV and a k_h of -7.9 mV. Experimental values in *Myxicola* ranged from -46 to -53 mV for V_h and -6.6 to -9.2 mV for k_h, for a large de-

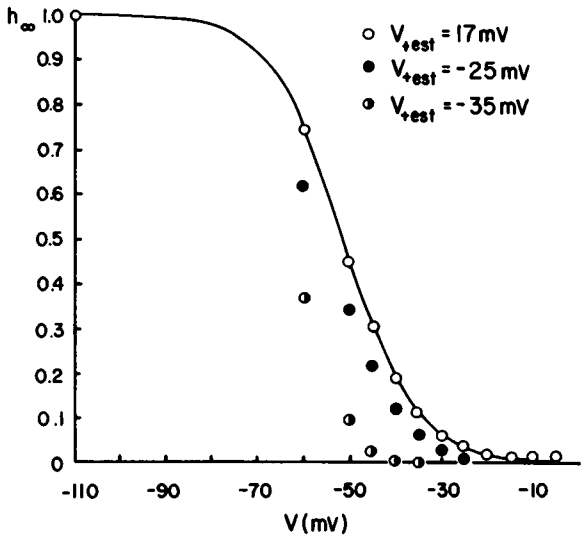

FIGURE 6

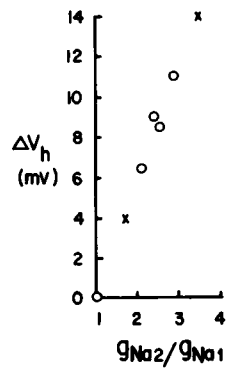

FIGURE 7

FIGURE 6 Computed value of the peak g_{Na} during a test pulse of 17 (open circles), −25 (filled circles), and −35 mV (half-filled circles), relative to the maximum g_{Na} attainable with each test pulse, h_∞, as a function of the potential during an 80 ms conditioning pulse. The solid line has been computed from $h_\infty = [1 + \exp(-51.5-V/-7.9)]^{-1}$.

FIGURE 7 Experimental values of the shift of the h_∞ curve as a function of the ratio of the peak g_{Na} of the two test pulses used (open circles). The X's indicate the shifts of the simulated curves in Fig. 6 from the solid line of Fig. 6.

polarizing test pulse. The open circles in Fig. 6 indicate the calculated h_∞ values for a 17 mV test pulse, where $g_{Na}/g_{Na_{max}}$ is unity. The filled circles indicate the computed h_∞ values for a test pulse of −25 mV, where $g_{Na}/g_{Na_{max}}$ is now about 0.59. There is a shift to the left, in agreement with the experimental findings. And, the shift is a simple translation along the voltage axis, also in agreement with the experimental findings (Goldman and Schauf, 1972).

The half-filled circles of Fig. 6 indicate the computed h_∞ values for a −35 mV test pulse, where $g_{Na}/g_{Na_{max}}$ is only about 0.29. There is a further shift to the left, again in agreement with the experimental findings. The shift is now not a simple translation along the voltage axis, the points for small h_∞ values falling somewhat too low. This discrepancy is very small, however, and is probably not detectable in the noise of an experimental determination. These h_∞ shifts are indicated by the x's of Fig. 7. The open circles of the Figure indicate the h_∞ shift values reported by Goldman and Schauf (1972).

Fig. 8 shows a computation of a conditioning pulse experiment in which a conditioning step of variable duration is followed by a step back to −50 mV of fixed duration and then by a test pulse. The computed results show a clear delay in the development of inactivation, in agreement with the experimental findings (Goldman and

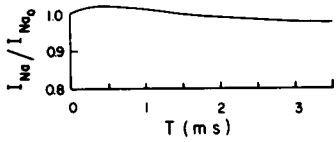

FIGURE 8

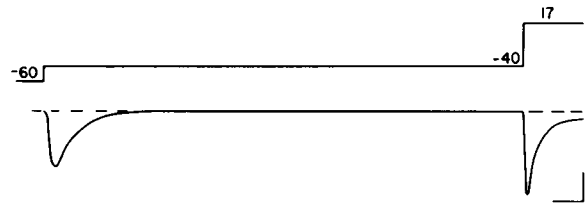

FIGURE 9

FIGURE 8 Computed value of the peak sodium current during a −20 mV test pulse, relative to the value with no conditioning pulse, I_{Na}/I_{Na_0}, as a function of the duration of a −5 mV conditioning pulse. The holding potential was −50 mV, and there was a step back to holding for 15 ms between each conditioning pulse and the test pulse.

FIGURE 9 Computed time course of the sodium current during a −40 mV conditioning pulse and a 17 mV test pulse. Scale: 40 mV, 0.05 mA/cm^2, 5 ms.

Schauf, 1972). Computations with smaller conditioning steps do show a longer delay, also in agreement with the experimental findings.

The computed inactivation curve is not monotonic, rising by nearly 2% of the value without a conditioning pulse before declining. This may be due to the somewhat greater steady-state occupancy of B at −50 mV for the simulations, as compared to −60 to −65 mV during the step back, experimentally. Such small effects should be very difficult to detect experimentally.

Fig. 9 shows a calculation of the time course of the I_{Na} during a −40 mV conditioning pulse, and again during the immediately subsequent 17 mV test pulse. Again in agreement with the experimental findings, the I_{Na} shuts off nearly entirely during the conditioning pulse, but rises up again during the test pulse.

In summary, the model presented here seems to be able to account quantitatively for all of the experimentally observed behavior of the g_{Na}. In addition, it is also possible to simulate the effects of internal perfusion with pronase (Armstrong, et al., 1973), by setting b equal to zero in Eq. 3 and reducing $\bar{g}'_{Na}$ by half (Goldman, 1975).

DISCUSSION

A view of the sodium gating machinery which is consistent with the observed behavior of the g_{Na}, is to imagine that the gate, in *Myxicola,* is composed of five independent subunits, each of the type illustrated in scheme I. The proposal of coupled activation-inactivation kinetics for the g_{Na}, first made by Hodgkin and Huxley (1952 *c*) has been considered by a number of other investigators (Mullins, 1959; Hoyt, 1963; Goldman, 1964; Chandler and Meves, 1970; Moore and Jakobsson, 1971; Peganov et al., 1973; Tredgold, 1973). More recently Bezanilla and Armstrong (1974) have interpreted some of their observations on sodium gating currents in terms of a coupled activation-inactivation process.

There are several other proposed models for the g_{Na}, however, which are inconsistent with the model presented here. In particular, all models in which the inactivation of

the g_{Na} is obligatorily coupled to the flow of the sodium current, as in the model of Offner (1972) and in the stored charge models of Hoyt and Strieb (1971) and Landowne (1972), seem to be ruled out. Rather, inactivation seems to arise as an internal property of the gating machinery.

I have also explored other, less generalized models for the g_{Na}. Of particular interest is the following pair of coupled first order differential equations:

$$\dot{\nu} = -K_1 \nu + K_2 U + K_4 - K_2 \tag{14}$$

$$\dot{U} = -K_4 U + K_5 \nu, \tag{15}$$

where K_1 to K_4 are functions of membrane potential only. The form of Eqs. 14 and 15 is consistent with the view that the gate subunit is of the type in scheme II:

$$A \underset{k_2}{\overset{k_1}{\rightleftharpoons}} B \underset{k_4}{\overset{k_3}{\rightleftharpoons}} C,$$

where A, B, C, ν, and U are all defined as before. As this model has only four parameters, the K's may be obtained immediately in terms of a, b, ν_∞, and $\dot{\nu}^*(0)$:

$$K_1 = a + b - [ab\nu_\infty/\dot{\nu}^*(0)], \tag{16}$$

$$K_2 = [ab\nu_\infty - (\dot{\nu}^*(0))^2]/\nu^*(0), \tag{17}$$

$$K_4 = ab\nu_\infty/\dot{\nu}^*(0), \tag{18}$$

$$K_5 = \frac{(ab\nu_\infty)(a + b - [ab\nu_\infty/\dot{\nu}^*(0)]) - ab\dot{\nu}^*(0)}{ab\nu_\infty - (\dot{\nu}^*(0))^2}. \tag{19}$$

Eqs. 14–19 could not reproduce the experimental observations. There was not a single set of parameters that could adequately simulate both the $g_{Na}/g_{Na_{max}}(V)$ curve of Fig. 3 and the normal $h_\infty(V)$ curve. h_∞ shifts could also not be produced with any set of parameters that were reasonably close to the experimental values. It seems that the C to A path of scheme I is an essential feature of the model.

Computations were also made using the Hoyt (1968) model:

$$\dot{\nu} = -K_1 U - K_3 \nu + K_4, \tag{20}$$

$$\dot{U} = -K_1 U + K_2. \tag{21}$$

These equations may be interpreted as a special case of scheme I with

$$k_3 = k_6 \tag{22}$$

$$k_1 = 2k_4 + k_5 + k_6. \tag{23}$$

Hoyt has presented two possible sets of definitions of the K's in terms of a, b, ν_∞,

and $\dot{\nu}^*(0)$ and computations were carried out using both sets. Results from both versions of the Hoyt model were quite similar. Qualitatively the Hoyt model did reproduce many of the experimental results, i.e., τ_c was greater than τ_h and, of course, there are h_∞ shifts. However the results were not quantitatively satisfactory, as might have been anticipated considering the arbitrariness of the assumptions of Eqs. 22 and 23.

Scheme I is not the only physical interpretation consistent with Eqs. 1, 4, and 5. It is possible to make a transformation of variables (see e.g. FitzHugh, 1969) to obtain the result

$$g_{Na} = \bar{g}'_{Na}(\theta + \phi)^5, \tag{24}$$

where θ and ϕ are independent first order variables having the property that the behavior of $(\theta + \phi)$ is identical to ν. In this framework the Hodgkin-Huxley model

$$g_{Na} = \bar{g}_{Na} m^3 h$$

may be viewed as a special or degenerate case of a second order variable, and the model presented here may be viewed as a generalization of Hodgkin-Huxley kinetics.

Physically, Eq. 24 may be interpreted as a non-coupled model in which there are five separate activation processes each of which is contravened by its own independent inactivation process. This is in contrast to Hodgkin-Huxley kinetics where the resultant activation process (itself composed of subunits) is contravened as a whole by the single inactivation process. I see no way to choose between the alternative formulations of Eqs. 1 and 24, mathematically. However, the physical picture suggested by Eq. 1 is simpler to envisage than the sort suggested by Eq. 24, as either θ or ϕ must be negative over at least some potential ranges. Also, the 10 independent processes of Eq. 24 ought to make for a noisier system.

Another view of the gating machinery results if the ν and U variables are no longer interpreted as the probabilities of occupancy of the conducting and inactivated states. These variables can also be interpreted as describing some continuously changing parameters of each individual gate subunit, e.g. the orientations of some molecular structures which occlude the channel mouth. In this case the time course of ν reflects the time course of opening and closing of each gate subunit. In the case represented by scheme I it is assumed that the time course of an individual transition between states is rapid relative to the time course of the g_{Na}, and that the occurrence of these transitions is distributed in time.

The new quantitative description of the g_{Na} presented here is probably the minimum formal description consistent with the experimental behavior, i.e., it is likely that all realistic models for the g_{Na} must be formally equivalent to Eqs. 1, 4, and 5. It also seems probable that the view of the gating subunit presented in scheme I is one useful guide, for the present, for the formulation of physical models for the g_{Na}.

I thank the many people who provided stimulating discussions and encouragement during the course of this work. I especially thank R. Hahin, R. B. Moreton, and P. K. Schofield, and also Dr. J. E. Treherne who kindly provided facilities during part of this project.

This work was supported in part by U. S. Public Health Service Research Grant NS 07734 and in part by U. S. Public Health Service Special Research Fellowship F10 NS 02696.

Received for publication 24 June 1974.

REFERENCES

ARMSTRONG, C. M. 1970. Comparison of g_K inactivation caused by quaternary ammonium ion with g_{Na} inactivation. *Biophys. Soc. Abstr.* **10**:185*a*.

ARMSTRONG, C. M., F. BEZANILLA, and E. ROJAS. 1973. Destruction of sodium conductance inactivation in squid axons perfused with pronase. *J. Gen. Physiol.* **62**:375.

BEZANILLA, F., and C. M. ARMSTRONG. 1974. Gating currents of the sodium channels: three ways to block them. *Science (Wash. D.C.).* **183**:753.

BINSTOCK, L., and L. GOLDMAN. 1969. Current and voltage-clamped studies on *Myxicola* giant axons: effect of tetrodotoxin. *J. Gen. Physiol.* **54**:730.

CHANDLER, W. K., A. L. HODGKIN, and H. MEVES. 1965. The effect of changing the internal solution on sodium inactivation and related phenomena in giant axons. *J. Physiol. (Lond.).* **180**:821.

CHANDLER, W. K., and H. MEVES. 1970. Evidence for two types of sodium conductance in axons perfused with sodium fluoride solution. *J. Physiol. (Lond.).* **211**:653.

FITZHUGH, R. 1969. Mathematical models of excitation and propagation in nerve. *In* Biological Engineering. H. P. Schwan, editor. McGraw-Hill, Inc., New York. 1.

FRANKENHAEUSER, B. 1959. Steady state inactivation of sodium permeability in myelinated nerve fibres of *Xenopus laevis*. *J. Physiol. (Lond.).* **148**:671.

FRANKENHAEUSER, B. 1963. Inactivation of the sodium carrying mechanism in myelinated nerve fibers of *Xenopus laevis*. *J. Physiol. (Lond.).* **169**:445.

GOLDMAN, D. E. 1964. A molecular structural basis for the excitation properties of axons. *Biophys. J.* **4**:167.

GOLDMAN, L. 1975. Pronase and models for the sodium conductance. *J. Gen. Physiol.* In press.

GOLDMAN, L., and L. BINSTOCK. 1969. Current separations in *Myxicola* Giant axons. *J. Gen. Physiol.* **54**:741.

GOLDMAN, L., and C. L. SCHAUF. 1972. Inactivation of the sodium current in *Myxicola* giant axons; evidence for coupling to the activation process. *J. Gen. Physiol.* **59**:659.

GOLDMAN, L., and C. L. SCHAUF. 1973. Quantitative description of sodium and potassium currents and computed action potentials in *Myxicola* giant axons. *J. Gen. Physiol.* **61**:361.

HASS, H. G., R. KERN, H. M. EINWACHTER, and M. TARR. 1971. Kinetics of Na inactivation in frog atria. *Pfluegers Arch. Eur. J. Physiol.* **323**:141.

HODGKIN, A. L., and A. F. HUXLEY. 1952*a*. Currents carried by sodium and potassium ions through the membrane of the giant axon of *Loligo*. *J. Physiol. (Lond.).* **116**:449.

HODGKIN, A. L., and A. F. HUXLEY. 1952*b*. The dual effect of membrane potential on sodium conductance in the giant axon of *Loligo*. *J. Physiol. (Lond.)* **116**:497

HODGKIN, A. L., and A. F. HUXLEY. 1952*c*. A quantitative description of membrane current and its applications to conduction and excitation in nerve. *J. Physiol. (Lond.).* **117**:500.

HOYT, R. C. 1963. The squid giant axon. Mathematical models. *Biophys. J.* **3**:399.

HOYT, R. C. 1968. Sodium inactivation in nerve fibers. *Biophys. J.* **8**:1074.

HOYT, R. C., and W. J. ADELMAN. 1970. Sodium inactivation. Experimental test of two models. *Biophys. J.* **10**:610.

HOYT, R. C., and J. D. STRIEB. 1971. A stored charge model for the sodium channel. *Biophys. J.* **11**: 868.

LANDOWNE, D. 1972. A new explanation of the ionic currents which flow during the nerve impulse. *J. Physiol. (Lond.).* **222**:46p.

MOORE, L. E., and E. JAKOBSSON. 1971. Interpretation of the sodium permeability changes of myelinated nerve in terms of linear relaxation theory. *J. Theor. Biol.* **33**:77.

MULLINS, L. J. 1959. An analysis of conductance changes in squid axon. *J. Gen. Physiol.* **42**:1013.

OFFNER, F. F. 1972. The excitable membrane. A physiochemical model. *Biophys. J.* **12**:1583.

PEGANOV, E. M. 1973. Kinetics of the process of inactivation of sodium channels in the node of Ranvier of frogs. *Bull. Exp. Biol. Med.* **76**:5.

PEGANOV, E. M., E. N. TIMIN, and B. I. KHODOROV. 1973. Interrelationship between the processes of sodium activation and inactivation. *Bull. Exp. Biol. Med.* **76**:7.

SCHAUF, C. L. 1974. Sodium currents in *Myxicola* axons. Nonexponential recovery from the inactive state. *Biophys. J.* **14**:151.

TREDGOLD, R. H. 1973. A possible mechanism for the negative resistance characteristic of axon membranes. *Nat. New Biol.* **242**:209.